Design of a Power-Spectrum-Based ATM Connection Admission Controller for Multimedia Communications

Chung-Ju Chang, *Senior Member, IEEE*, Chih-Hen Lin, Dah-Sheng Guan, and Ray-Guang Cheng, *Member, IEEE*

***Abstract*— This paper proposes a power-spectrum-based connection admission controller design in asynchronous transfer mode (ATM) switches for multimedia communications. The controller contains a power-spectrum-indexed table for managing multimedia call requests, where traffic characteristics of call requests are described by the power spectrum. The power spectrum can be obtained from the claimed traffic parameters of peak rate, mean rate, and peak rate duration; the power spectrum has been shown to have a dominant effect on system performance. The results show that the proposed power-spectrum-based connection admission control method achieves higher system utilization and lower call-blocking probability than the equivalent-capacity allocation method.**

***Index Terms*—Asynchronous transfer mode, connection admission control, multimedia communications, power spectrum.**

I. Introduction

ASYNCHRONOUS transfer mode (ATM) is considered to be the foundation on which broad-band Integrated Services Digital Networks (B-ISDN) are built [1], [2]. ATM systems have the advantage of flexibility and efficiency in accommodating multimedia services that possess different traffic characteristics and quality-of-service (QoS) requirements. However, ATM switches require a sophisticated connection admission control method, so as not only to satisfy distinct QoS requirements, but also to enhance system utilization.

An equivalent-capacity allocation method has been proposed [3]. These studies on resource allocation and management for ATM switches assumed that voice sources were modeled by a two-state Markov-modulated deterministic process (MMDP), video sources were modeled by a multiple-state birth–death Markov-modulated Poisson process (MMPP), and data sources were modeled by a Poisson process [4]–[6]. Markov-modulated arrival processes have correlation characteristics that significantly affect system performance (e.g., blocking probability and throughput) of ATM switches. Therefore, in designing an ATM connection admission controller for multimedia communication, it is necessary to thoroughly consider this correlation function.

Li *et al.* [7]–[10] studied a high-speed network from the frequency domain of input traffic. They found that the correlation function can be captured by second-order and higher order statistics, such as power spectrum, bispectrum, and trispectrum, and the second-order power spectrum has a much more significant effect on the system performance than any high-order statistics.

In this paper, we designed an ATM connection admission controller for multimedia calls (voice, video, and data) based on the power spectra of the cell arrival process of calls. We constructed a connection admission control table that contained the performance measure of cell loss probability versus parameters of bell-shaped power spectrum of voice/video (real-time) calls and arrival rates of data (nonreal-time) calls. When a new real-time call comes to an ATM switch, the connection admission controller in the switch first estimates the power spectrum of the new incoming call from the negotiated parameters of peak rate, mean rate, and peak rate duration, adds the power spectrum of the new call to the power spectrum of existing calls, and then obtains a bell-shaped power spectrum. With the parameters of the approximated bell-shaped power spectrum, the connection admission controller obtains the cell loss probability of the new real-time call by looking up the connection admission control table and then accepts or rejects the new real-time call. Similarly, when a new nonreal-time call comes to the switch, the connection admission controller estimates the traffic load of the existing calls and then judges whether to accept or reject the new nonreal-time call according to its cell loss probability. The results show that our power-spectrum-based connection admission control method achieves higher system utilization and lower call-blocking probabilities than the equivalent-bandwidth allocation method proposed by Guérin, Ahmadi, and Naghshineh [3].

This paper is organized as follows. In Section II, we depict the system diagram of an ATM switch and describe the power spectrum of Markov-modulated input processes for multimedia services. In Section III, we describe our design for the power-spectrum-based connection admission controller, including the

Manuscript received October 13, 1996; revised July 20, 1997. This work was supported in part by the National Science Council, Taiwan, R.O.C., under Contract NSC 84-2213-E009-137.

C.-J. Chang and R.-G. Cheng are with the Department of Communication Engineering and Center for Telecommunications Research, National Chiao Tung University, Hsinchu, 300 Taiwan, R.O.C.

C.-H. Lin was with the Department of Communication Engineering and Center for Telecommunications Research, National Chiao Tung University, Hsinchu, 300 Taiwan, R.O.C. He is now with the Switching Technology Department, Chunghwa Telecommunication Laboratories, Chungli, Taiwan, R.O.C.

D.-S. Guan was with the Department of Communication Engineering and Center for Telecommunications Research, National Chiao Tung University, Hsinchu, 300 Taiwan, R.O.C. He is now with the Network Planning Department, Chunghwa Telecommunication Laboratories, Chungli, Taiwan, R.O.C.

Publisher Item Identifier S 0278-0046(98)00410-9.

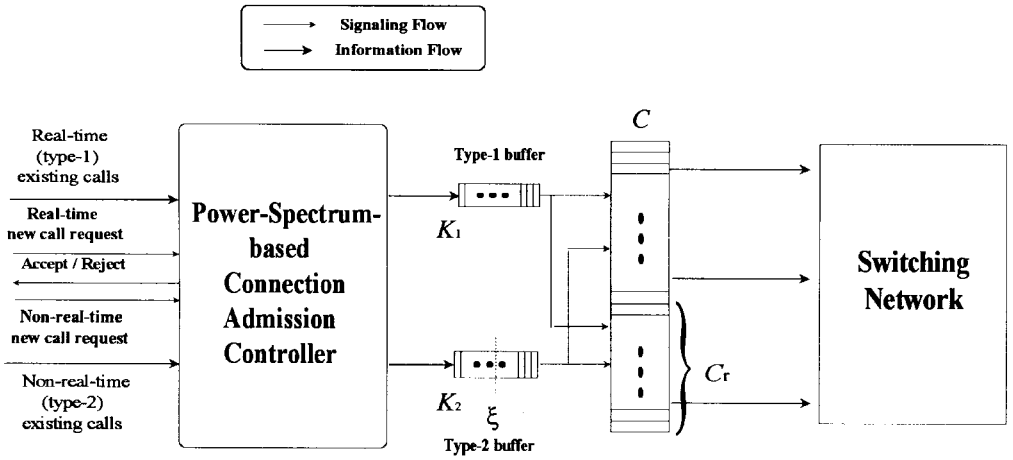

Fig. 1. The conceptual diagram of an ATM switch.

establishment of the connection admission control table, for multimedia communications. The simulation results and discussions are given in Section IV. The concluding remarks are presented in Section V.

II. System Configuration and Input Power-Spectrum

The conceptual diagram of an ATM switch containing the power-spectrum-based connection admission controller is shown in Fig. 1. We classify the multimedia calls input to the ATM switch into real-time voice/video (type-1) and nonreal-time data (type-2) traffic. Input messages from both types of traffic are segmented into fixed-length ATM cells and the constant service time of an ATM cell is referred as a frame time period T. The switch provides two buffers with capacities K_1 and K_2 for type-1 and type-2 traffic, respectively, and it has C parallel synchronous links (servers) connected to the switching network. The C parallel synchronous links are operated in a slot-by-slot fashion. A *queue-length-threshold* (QLT) link capacity assignment policy [11], [12] is adopted, which is noted as follows. If the queue length of type-2 traffic is higher than or equal to a threshold value ξ, C_r links are reserved for type-2 traffic and the remaining $(C - C_r)$ links are first accessed by type-1 traffic and then accessed by type-2 traffic; if the queue length of type-2 traffic is less than ξ, the total C links are first allocated to type-1 traffic and type-2 traffic can only utilize the remaining links. The service discipline in each buffer is first-come-first-serve (FCFS).

We use a two-state MMDP to model the cell-arrival process of an incoming voice call. As shown in Fig. 2(a), γ and 0 are the cell-arrival rates when the voice source is at "on" state and "off" state, respectively; α and β are the transition rates for the two-state Markov chain. We model the cell-arrival process of an incoming video call by a superposition of N independent and identical two-state MMPP's with cell-arrival rate ν at "on" state, the cell-arrival rate 0 at "off" state, and transition rates of $\hat{\alpha}$ and $\hat{\beta}$. Fig. 2(b) shows the video source model for an $(N+1)$-state MMPP, and we use an independent Poisson arrival process with a mean rate of γ_D for the cell-arrival process of an incoming data call. All the voice, video, and

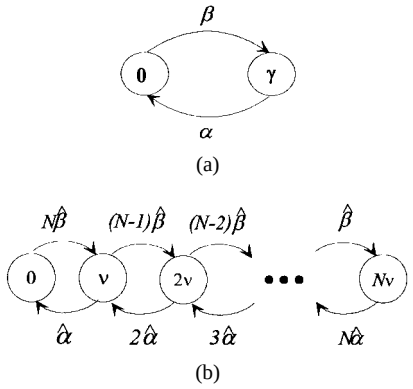

Fig. 2. (a) Voice source: a two-state MMDP. (b) Video source: $(N+1)$-state MMPP.

data call-arrival processes are assumed to be independently Poisson distributed.

Denote $\boldsymbol{Q}$ as the transition-rate matrix of an MMPP input video traffic to the switch, and $\boldsymbol{Q}$ can be represented as

$$\boldsymbol{Q} = \sum_{l=0}^{N} \lambda_l \boldsymbol{g}_l \boldsymbol{h}_l \tag{1}$$

where λ_l is the eigenvalue of $\boldsymbol{Q}, \boldsymbol{g}_l$, and $\boldsymbol{h}_l$ are the associated right and left eigenvectors of $\boldsymbol{Q}$, respectively, and $(N+1)$ is the number of states in the MMPP [7]. The autocorrelation function $R(\tau)$ and its corresponding power spectrum $P(\omega)$ of the input process can be obtained by [7]

$$R(\tau) = \overline{\gamma}\delta(\tau) + \psi_0 + \sum_{l=1}^{N} |\psi_l| e^{\mathrm{Re}\{\lambda_l\}|\tau|} \cdot \cos(\mathrm{Im}\{\lambda_l\}|\tau| + \arg\{\psi_l\}) \tag{2}$$

and

$$P(\omega) = \overline{\gamma} + 2\pi\psi_0\delta(\omega) + \sum_{l=1}^{N} b(\omega - \omega_l) \tag{3}$$

where $\mathrm{Im}\{\cdot\}, \mathrm{Re}\{\cdot\}$, and $\arg(\cdot)$ denote the imaginary part, the real part, and the phase of the argument, respectively; $\overline{\gamma}$ is the mean arrival rate of the MMPP, which is given by

$$\overline{\gamma} = \sum_{i=0}^{N} \gamma_i \pi_i \tag{4}$$

where γ_i is the MMPP arrival rate in state i, and π_i is the steady-state probability in state i; $\delta(\tau)$ is defined as

$$\delta(\tau) = \begin{cases} \infty, & \tau = 0 \\ 0, & \text{otherwise.} \end{cases} \tag{5}$$

ψ_0 is the dc component given by

$$\psi_0 = \overline{\gamma}^2. \tag{6}$$

ψ_l is the average power contributed by λ_l and is given by

$$\psi_l = \sum_i \sum_j \pi_i \gamma_i \gamma_j g_{li} h_{lj}, \qquad \text{for } 1 \le l \le N. \tag{7}$$

g_{li} and h_{lj} are the ith and jth entities of the vectors $\boldsymbol{g_l}$ and $\boldsymbol{h_l}$, respectively; $b(\omega - \omega_l)$ is the bell function given by

$$\begin{aligned} b(\omega - \omega_l) &= \frac{-2\psi_l \,\mathrm{Re}\{\lambda_l\}}{(\mathrm{Re}\{\lambda_l\})^2 + (\omega - \omega_l)^2} \\ &= \frac{\psi_l B_{Wl}}{(B_{Wl}/2)^2 + (\omega - \omega_l)^2}, \quad \text{for } \lambda_l \neq 0 \end{aligned} \tag{8}$$

and

$$\frac{1}{2\pi} \int_{-\infty}^{+\infty} b(\omega - \omega_l)\, d\omega = \psi_l. \tag{9}$$

B_{Wl} is defined as the half-power bandwidth of a bell-shaped function corresponding to the eigenvalue λ_l and the derivation of $B_{Wl} = -2\,\mathrm{Re}\{\lambda_l\}$ can be found in Appendix A; ω_l is the central frequency of the bell-shaped function $b(\omega)$ defined as

$$\omega_l = \mathrm{Im}\{\lambda_l\}. \tag{10}$$

Equation (3) shows that the transition-rate matrix $\boldsymbol{Q}$ of an MMPP has a power spectrum $P(\omega)$ consisting of a white noise $\overline{\gamma}$, a dc component $2\pi\psi_0\delta(\omega)$, and a set of bell-shaped functions $b(\omega - \omega_l)$ the position of which is centered at $\omega = \omega_l$. The white noise results from from the Poisson local dynamics of the MMPP.

As far as the MMDP voice traffic is concerned, the Markovian property of the Markov chain still generates the bell-shaped functions and the dc component, but the deterministic rate process in the state of the Markov chain generates another dc component, instead of white noise.

Li and Huang in [7] showed that the influence of the white noise on the queueing behavior of a system was negligible. Therefore, in this paper, we only considered the dc component ψ_0, the average power ψ_l, and the half-power bandwidth B_{Wl} of the bell-shaped functions $b(\omega - \omega_l)$ as parameters for the power-spectrum-based connection admission control method.

The eigenvalues of the birth–death Markov chain, as shown in Fig. 2, are all real and the bell-shaped functions are centered at $\omega_l = 0$. The zero-centered bell-shaped functions of the input power spectrum have a significant effect on the system performance. For detailed studies, see [7] and [8].

When a new voice-call request arrives, its traffic parameters of peak rate, mean rate, and peak-rate duration, denoted by γ_p, γ_m, and d_p, respectively, are given by negotiation. Based on the voice model shown in Fig. 2(a), we can then determine the arrival rate γ and the transition rates α and β of the two-state MMDP by

$$\gamma = \gamma_p \tag{11}$$

$$\alpha = \frac{1}{d_p} \tag{12}$$

and

$$\beta = \frac{\gamma_m}{d_p(\gamma_p - \gamma_m)}. \tag{13}$$

When a new video-call request with $(\gamma_p, \gamma_m, d_p)$ arrives, we can also obtain the arrival rate ν and the transition rates $\hat{\alpha}$ and $\hat{\beta}$ of the $(N+1)$-state MMPP, as shown in Fig. 2(b), by

$$\nu = \frac{\gamma_p}{N} \tag{14}$$

$$\hat{\alpha} = \frac{1}{N d_p} \tag{15}$$

and

$$\hat{\beta} = \frac{\gamma_m}{N d_p(\gamma_p - \gamma_m)}. \tag{16}$$

The detailed derivation of the transition rate $\hat{\beta}$ is given in Appendix B.

We then have the corresponding input power spectrum characterized by parameters ψ_0, ψ_l, and $B_{Wl}, 1 \le l \le N$, as given in (6)–(8). Note that, for the $(N+1)$-state MMPP video-source model contributed by N independently identically distributed (i.i.d.) two-state Markov chains, $\psi_1 = \psi_2 = \cdots = \psi_N$, and the bell-shaped functions are all zero centered.

III. Power-Spectrum-Based Connection Admission Control

We describe the design of the proposed power-spectrum-based connection admission controller and the construction of the power-spectrum-based connection admission control table here. A new call is assumed to be accepted if the ATM switch can satisfy QoS requirements of cell loss probability for new and existing calls. If the requirement cannot be satisfied, the incoming call is rejected.

A. Power-Spectrum-Based Connection Admission Controller

The functional block diagram of the power-spectrum-based connection admission controller is shown in Fig. 3. Whenever a new voice or video real-time call comes to the switch, the *power spectrum estimator* computes the arrival rate and the transition rates of the Markov modulated arrival process (MMDP or MMPP) and estimates the power spectrum from the

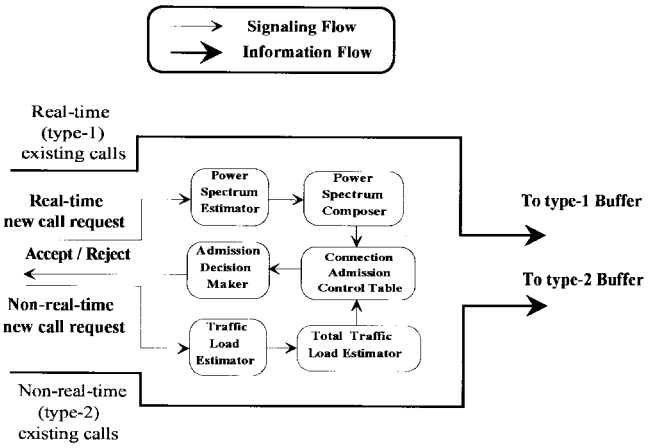

Fig. 3. The functional block diagram of the power-spectrum-based connection admission controller in an ATM switch.

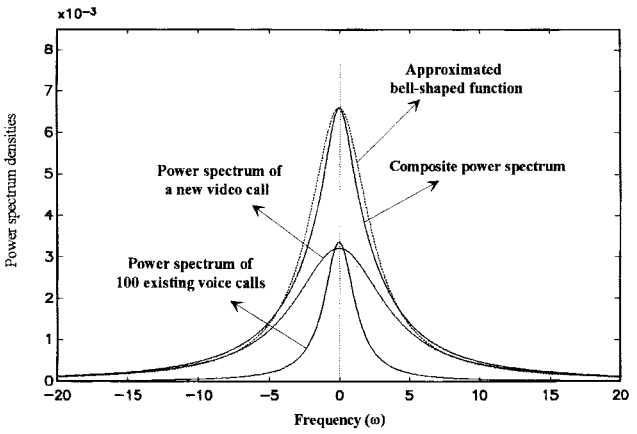

Fig. 4. An example of the approximated bell-shaped function obtained from a composite power spectrum.

negotiated traffic parameters $(\gamma_p, \gamma_m, d_p)$. The *spectrum composer* adds the power spectrum of the new call to the power spectrum of existing calls and obtains a composite power spectrum. This composite power spectrum is approximated by a bell-shaped function. (Fig. 4 shows an example of an approximated bell-shaped function representing the composite power spectrum obtained from the power spectrum of 100 existing voice calls in progress and one new video call in call setup.) Consequently, the cell-loss probability of the new real-time call can then be found by looking up the *connection admission control table*. (The establishment of the power-spectrum-based connection admission control table will be described later.) The *admission decision maker* accepts the new call if cell-loss probability satisfies its QoS requirement, otherwise it rejects the new call.

When a new nonreal-time data call requests to enter the switch, the *traffic load estimator* obtains the traffic load intensity $\gamma_D T/C$ of the new call according to its mean arrival rate γ_D. The *total traffic load estimator* adds the load of the new call to the load of existing nonreal-time calls and obtains the overall traffic intensity $\Gamma_D T/C$. The cell-loss probability of the type-2 traffic can be found by looking it up in the the *connection admission control table*, and the *admission decision maker* accepts the new call if the cell-loss probability satisfies its QoS requirement, otherwise it rejects the new call.

Here, we elaborate on how to approximate the composite power spectrum by a bell-shaped function in the spectrum composer. As (8) implies, a zero-centered bell-shaped function can be characterized by its average power and half-power bandwidth. We let the approximated bell-shaped function of the composite power spectrum possess the same value at $\omega = 0$ and the same average power as those of the composite power spectrum. We denote the dc component and the approximated bell-shaped function of the composite power spectrum by ψ_{a0} and $b_a(\omega)$ and denote the average power and the half-power bandwidth of $b_a(\omega)$ by ψ_a and B_{Wa}. The power spectrum of existing calls is assumed to have a dc component ψ_{e0} and an approximated bell-shaped function $b_e(\omega)$ with average power ψ_e and half-power bandwidth B_{We}; the power spectrum of a new call obtained from the negotiation parameters $(\gamma_p, \gamma_m, d_p)$ also has a dc component ψ_{n0} and an approximated bell-shaped function $b_n(\omega)$ with average power ψ_n and half-power bandwidth B_{Wn}. Therefore, ψ_{a0}, ψ_a, and $B_{Wa}(\omega)$ can be respectively obtained by

$$\psi_{a0} = (\sqrt{\psi_{e0}} + \sqrt{\psi_{n0}})^2 \tag{17}$$

$$\psi_a = \psi_e + \psi_n \tag{18}$$

and

$$B_{Wa} = \frac{\psi_a B_{We} B_{Wn}}{\psi_e B_{Wn} + \psi_n B_{We}}. \tag{19}$$

Equation (19) is derived from $b_a(\omega) = b_e(\omega) + b_n(\omega)$ at $\omega = 0$. Such an assumption would cause the approximated bell-shaped function to contain more low-frequency component power and result in an overestimation of type-1 cell-loss probability in the construction of the connection admission control table.

B. Establishment of the Power-Spectrum-Based Connection Admission Control Table

The power-spectrum-based connection admission control table contains cell-loss probabilities of type 1 and type 2 (CLP1 and CLP2) versus ψ_{a0}, ψ_a, and B_{Wa} of zero-centered bell-shaped functions of type-1 traffic and Γ_D of type-2 traffic. We use simulations to obtain CLP1 and CLP2. The simulation model for obtaining CLP1 for a given $\psi_{a0}, \psi_a, B_{Wa}$, and Γ_D is the same as that defined in Fig. 1, which adopts QLT policy and has system parameters of K_1, K_2, C_r, and ξ. The input process of type-2 data traffic is assumed to be a Poisson process with an arrival rate of Γ_D. The input process of type-1 voice (or video) traffic is assumed to be two-state $((N+1)$-state) Markov chains with arrival rates of γ (or ν) and transition rates of α and β (or $\hat{\alpha}$ and $\hat{\beta}$) obtained from parameters of ψ_{a0}, ψ_a, and B_{Wa} of a zero-centered bell-shaped function given by

$$\gamma \text{ (or } \nu) = \frac{\psi_{a0} + \psi_a}{\sqrt{\psi_{a0}}} \tag{20}$$

$$\alpha \text{ (or } \hat{\alpha}) = \frac{\psi_a B_{Wa}}{2(\psi_{a0} + \psi_a)} \tag{21}$$

and

$$\beta \text{ (or } \hat{\beta}) = \frac{\psi_{a0} B_{Wa}}{2(\psi_{a0} + \psi_a)}. \tag{22}$$

On the other hand, the simulation model for obtaining CLP2 is a system that adopts QLT policy and has a Poisson process with an arrival rate of Γ_D, a buffer size of K_2, and C_r total available links. Here, the QLT policy is modified. If the queue length is equal to or greater than ξ, all C_r links are available; otherwise, no links are accessible. This model differs from the one shown in Fig. 1, in which type-2 traffic can use at least C_r links whenever the queue length is equal to or greater than ξ. Hence, the cell-loss probability of type-2 traffic in the table is also overestimated.

The procedures for establishing the power-spectrum-based connection admission control table cac_table( ) are described in the following.

```
FUNCTION cac_table( )
BEGINFUNC
    Initialize the values of traffic load Γ_D for type-2
      traffic and dc component ψ_a0,
      average power ψ_a, and half-power bandwidth
      B_Wa for type-1 traffic
    Set the desired ranges of Γ_D, ψ_a0, ψ_a, and B_Wa
    Set the increments steps of ΔΓ_D, Δψ_a0, Δψ_a,
      and ΔB_Wa
    For Γ_D within the desired range of traffic load
      Call type-2_simulation (Γ_D)
      For B_Wa within the desired range of bandwidth
        For ψ_a within the desired range of average
          power
          For ψ_a0 within the desired range of dc
            component
            Call power-spectrum_to_2-state-MC
              (B_Wa, ψ_a, ψ_a0)
            Call type-1_simulation (Γ_D, γ, α, β)
            Write to cac_table with format
              (Γ_D, B_Wa, ψ_a, ψ_a0, CLP2, CLP1)
            Increase ψ_a0 by Δψ_a0
          EndFor
        Increase ψ_a by Δψ_a
        EndFor
      Increase B_Wa by ΔB_Wa
      EndFor
    Increase Γ_D by ΔΓ_D
    EndFor
ENDFUNC
```

```
FUNCTION type-2_simulation (Γ_D)
BEGINFUNC
    Generate type-2 traffic according to a Poisson
      process with mean rate Γ_D
    Simulate the system described in the second
      paragraph of this subsection that has K_2
      buffer size, C_r
      available links, and ξ queue-length-threshold.
    Calculate the CLP2
    Return CLP2
ENDFUNC
```

```
FUNCTION power-spectrum_to_2-state-MC
  (B_Wa, ψ_a, ψ_a0)
BEGINFUNC
Calculate the mean arrival rate in on-state γ,
  the on-off transition rate α, and the off-on
  transition rate β,
  from parameters B_Wa, ψ_a, ψ_a0, according to
  (20), (21), and (22)
Return γ, α, β
ENDFUNC
FUNCTION type-1_simulation (Γ_D, γ, α, β)
BEGINFUNC
Generate type-1 input traffic according to a 2-state
  Markov process with parameters γ, α, β
Generate type-2 input traffic according to
  the Poisson process with mean rate γ_D
Simulate the system described in the first paragraph
  of this subsection that adopts the QLT scheduling
  policy and has system parameters of
  K_1, K_2, C_r, and ξ.
Calculate CLP1
Return CLP1
ENDFUNC
```

■

IV. Simulation Examples and Discussions

In the simulations, the system parameters were given by the buffer sizes $K_1 = K_2 = 100$, the total number of links $C = 20$, the number of reserved links $C_r = 10$, and the queue-length threshold of the QLT policy $\xi = 80$. For simplicity, the QoS requirement of cell-loss probability was assumed to be 10^{-3} for voice service, 10^{-5} for video service, and 10^{-6} for data service. We considered several simulation examples, but showed only an example in which a switch supports multimedia services of voice, video, and data calls.

In the example, the call parameters were defined as follows: call arrival rates for voice, video, and data were 10.115, 0.0743, and 0.4246 calls/s; the call holding time for voice, video, and data were 1, 5, and 30 s; and the peak rate γ_p was 64 kb/s, the mean rate γ_m was 27.6 kb/s, and the peak duration d_p was 1.366 s for a voice call. γ_p was 6 Mb/s, γ_m was 2.04 Mb/s, and d_p was 3.86 s for a video call. The arrival rate Γ_D for a data call was 9.0 cells/slot. We compared results with the system using the equivalent-capacity allocation method proposed in [3], under the same call parameters mentioned above.

Fig. 5(a) shows the number of accepted voice calls versus time. In it, we can see that the number of accepted voice calls using both control methods is similar. Fig. 5(b) shows the voice-call-blocking probability versus time. It shows that the power-spectrum-based control method outperforms the equivalent-capacity allocation method. Fig. 5(c) shows that the number of accepted data calls for both control methods is also similar. Fig. 5(d) shows the number of accepted video calls versus time. We can see that the system using the power-spectrum-based control method can accommodate more video calls than the one using the equivalent-capacity

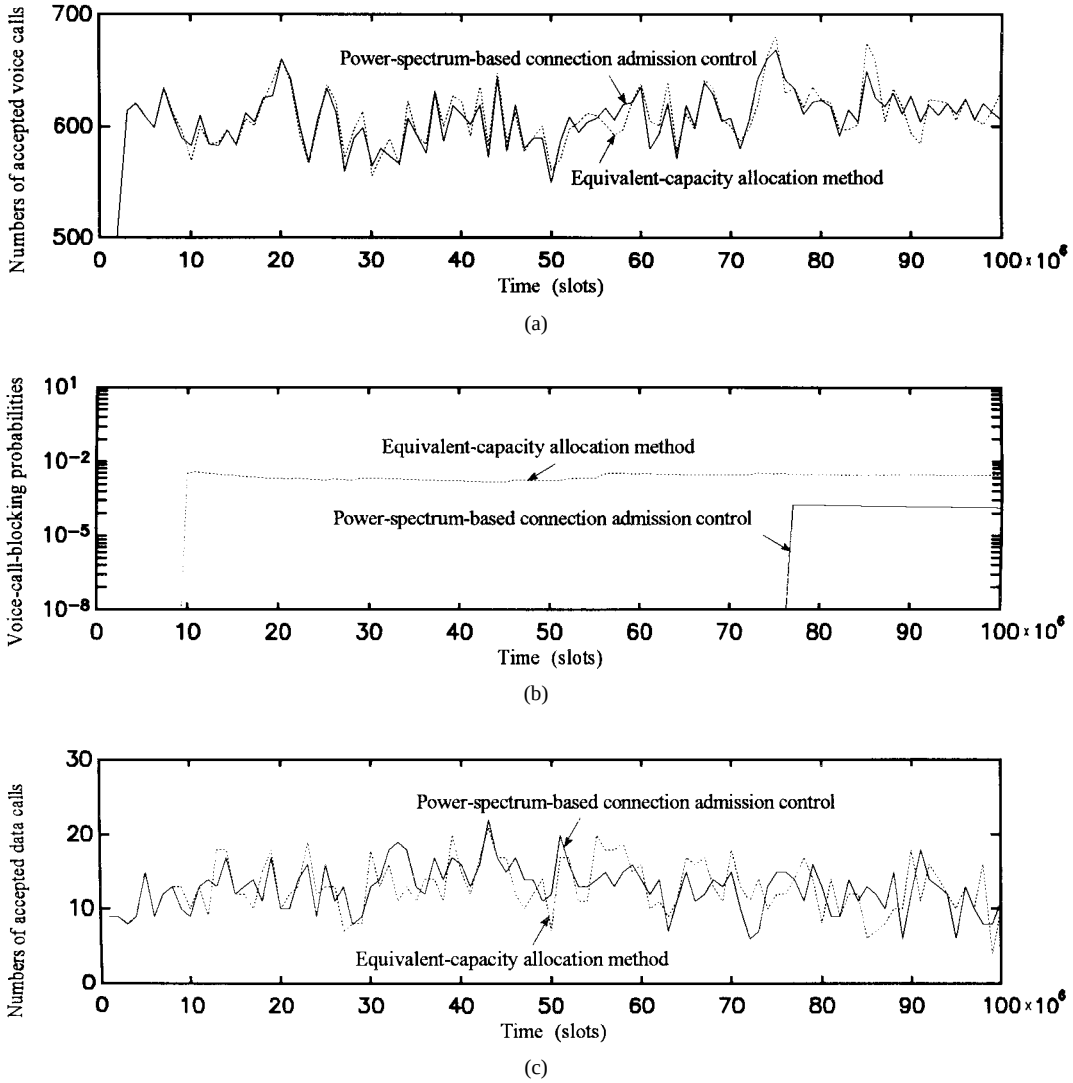

Fig. 5. (a) Number of accepted voice calls versus time. (b) Voice-call-blocking probabilities versus time. (c) Number of accepted data calls versus time.

allocation method. Fig. 5(e) shows the video-call-blocking probability versus time. It also reveals that the system using the power-spectrum-based control method has a lower video-call-blocking probability than the one using equivalent-capacity allocation method, and Fig. 5(f) shows overall system utilization versus time. In the simulations, the cell-loss probabilities are all zero using both methods. It shows that the power-spectrum-based connection admission control method can achieve 9% greater system utilization than the equivalent-bandwidth allocation method. Therefore, the power-spectrum-based connection admission control method is more efficient than the equivalent-capacity allocation method, because the former method takes the correlation (second-order statistics) effect of cell-arrival process into account.

V. Concluding Remarks

This paper has designed a power-spectrum-based connection admission controller for ATM switches in multimedia communication applications. Such a power-spectrum-based connection admission controller in the switch takes the correlation characteristics (second-order statistics) of cell-arrival processes into account. Whether an incoming call is accepted by a switch is determined by whether the cell-loss probability, obtained by reference to a power-spectrum-based connection admission control table, satisfies the QoS requirement or not. We presented a procedure for establishing the power-spectrum-based connection admission control table which contains the cell-loss probability indexed by type-1 traffic power-spectrum parameters and type-2 traffic arrival rate. In order to simplify the lookup table, we approximated the composite power spectrum, which is the sum of the power spectra of existing calls and new incoming calls, as a bell-shaped function. The results show that the system using the power-spectrum-based connection admission control method achieves a 9% higher utilization than the one using the equivalent-capacity allocation method [3].

In a real ATM network, where many ATM nodes are included, the CAC should be made for the global decision, instead of the local decision studied in this paper. Because the acceptance or rejection of the global decision is determined by the local decision of each node traversed by the call, the scheme we proposed can be extended to the global decision.

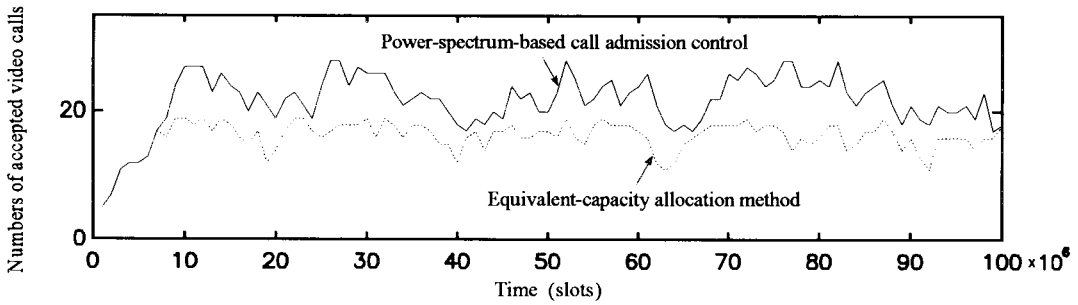

(d)

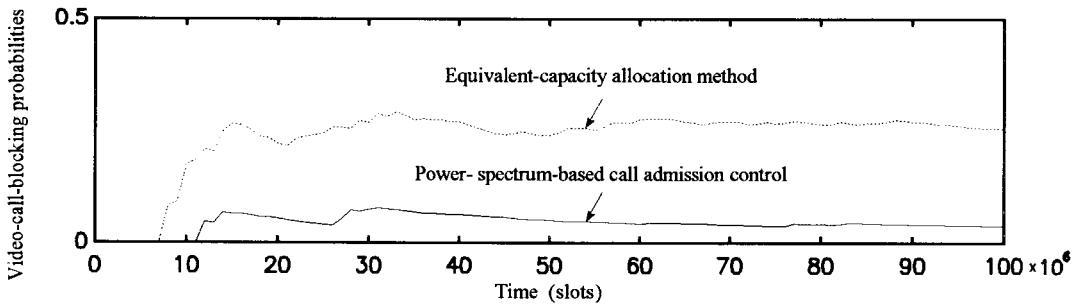

(e)

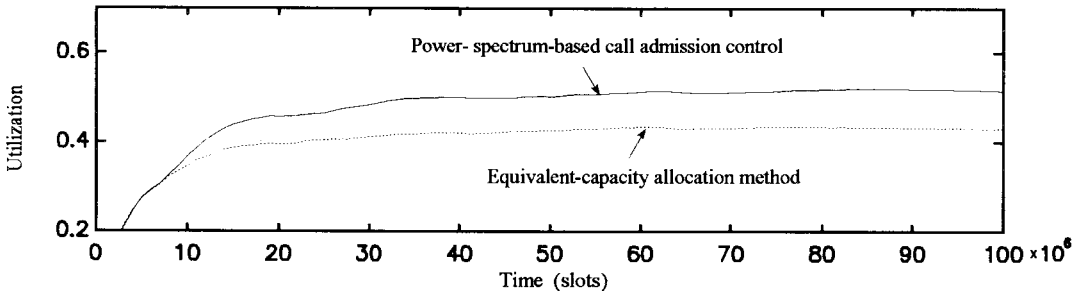

(f)

Fig. 5. *(Continued.)* (d) Number of accepted video calls versus time. (e) The video-call-blocking probabilities versus time. (f) The overall system utilization versus time, for a switch that accepts voice, data, and video calls.

APPENDIX A

Consider a bell-shaped power spectrum $b(w - w_l)$ with a half-power bandwidth B_{Wl}. From (8) and (9), B_{Wl} must satisfy

$$\begin{aligned}\frac{1}{2\pi}\int_{\omega_l - B_{Wl}}^{\omega_l + B_{Wl}} b(\omega - \omega_l)\, d\omega &= \frac{1}{2\pi}\int_{\omega_l - B_{Wl}}^{\omega_l + B_{Wl}} \frac{-2\psi_l \operatorname{Re}\{\lambda_l\}}{(\operatorname{Re}\{\lambda_l\})^2 + (\omega - \omega_l)^2}\, d\omega \\ &= \frac{\psi_l}{2}. \end{aligned} \tag{A1}$$

We can then find B_{Wl} from (A1), which is given by

$$B_{Wl} = -2\operatorname{Re}\{\lambda_l\}. \tag{A2}$$

■

APPENDIX B

We know that the steady-state probability of the $(N+1)$-state MMPP constructed by N i.i.d. two-state Markov chain is binominally distributed. The probability that there are k two-state Markov chains in the "on" state, $k = 0, 1, \cdots, N$, is given by

$$P(k) = \binom{N+1}{k} \hat{\epsilon}^k (1 - \hat{\epsilon})^{N+1-k} \tag{B1}$$

where $\hat{\epsilon}$ is defined as

$$\hat{\epsilon} = \frac{\hat{\beta}}{\hat{\alpha} + \hat{\beta}}. \tag{B2}$$

Therefore, we can have the mean rate γ_m of the $(N+1)$-state MMPP by

$$\gamma_m = N\hat{\alpha}\nu. \tag{B3}$$

Using (14), (15), and (B3), we can obtain the transition rate $\hat{\beta}$ by

$$\hat{\beta} = \frac{\gamma_m}{N d_p(\gamma_p - \gamma_m)}. \tag{B4}$$

■

REFERENCES

[1] R. Händel and M. M. Huber, *Integrated Broadband Networks: An Introduction to ATM-Based Networks*. Reading, MA: Addison-Wesley, 1991, p. 14.

[2] "Traffic control and congestion control in B-ISDN," International Telecommunications Union-Telecommunications, Geneva, Switzerland, ITU-T: Recommendation I.371, May 1996.

[3] R. Guérin, H. Ahmadi, and M. Naghshineh, "Equivalent capacity and its application to bandwidth allocation in high-speed networks," *IEEE J. Select. Areas Commun.*, vol. 9, pp. 968–981, Sept. 1991.

[4] J. N. Daigle and J. D. Langford, "Models for analysis of packet voice communications systems," *IEEE J. Select. Areas Commun.*, vol. SAC-4, pp. 856–868, Sept. 1986.

[5] H. Heffes and D. M. Lucantoni, "A Markov modulated characterization of packetized voice and data traffic and related statistical multiplexer performance," *IEEE J. Select. Areas Commun.*, vol. SAC-4, pp. 856–868, Sept. 1986.

[6] B. Maglaris , D. Anastassiou, P. Sen, G. Karlsson, and J. Robbins, "Performance analysis of statistical multiplexing for packet video sources," *IEEE Trans. Commun.*, vol. 36, pp. 834–844, July 1988.

[7] S. Q. Li and C. L. Hwang, "Queue response to input correlation functions: continuous spectral analysis," *IEEE Trans. Commun.*, vol. 41, pp. 678–692, Dec. 1993.

[8] ———, "Queue response to input correlation functions: discrete spectral analysis," *IEEE/ACM Trans. Networking*, vol. 1, pp. 522–533, Oct. 1993.

[9] S. Q. Li, S. Chong, and C. L. Hwang, "Link capacity allocation and network control by filtered input rate in high speed networks," *IEEE/ACM Trans. Networking*, vol. 3, pp. 10–25, Feb. 1995.

[10] H. D. Sheng and S. Q. Li, "Second order effect of binary sources on characteristics of queue and loss rate," in *Proc. IEEE INFOCOM*, Apr. 1993, pp. 18–27.

[11] C. J. Chang, P. C. Lin, and J. M. Chen, "Study on optimal queue-length-threshold scheduling policy for an ATM multiplexer with finite buffers and batch Poisson arrivals," *Comput. Networks ISDN Syst.*, no. 26, pp. 524–540, 1994.

[12] R. Chipalkatti, J. F. Kurose, and D. Towsley, "Scheduling policies for real-time and nonreal-time traffic in a statistical multiplexer," in *Proc. IEEE INFOCOM*, 1989, pp. 774–783.

Chung-Ju Chang (S'81–M'85–SM'94) was born in Taiwan, R.O.C., in 1950. He received the B.E. and M.E. degrees in electronics engineering from National Chiao Tung University, Hsinchu, Taiwan, R.O.C., in 1972 and the Ph.D degree in electrical engineering from National Taiwan University, Taiwan, R.O.C., in 1985.

From 1976 to 1988, he was with Telecommunication Laboratories, Directorate General of Telecommunications, Ministry of Communications, Taiwan, R.O.C., as a Design Engineer, Supervisor, Project Manager, and then Division Director. He was involved in designing digital switching system, RAX trunk tester, ISDN user–network interface, and ISDN service and technology trials in the Science-Based Industrial Park. He also acted as a Science and Technical Advisor for the Minister of the Ministry of Communications from 1987 to 1989. In August 1988, he joined the faculty of the Department of Communication Engineering and Center for Telecommunications Research, College of Electrical Engineering and Computer Science, National Chiao Tung University, Hsinchu, Taiwan, R.O.C., where he is currently a Professor and also an Advisor for the Ministry of Education. He was Director of the Institute of Communication Engineering from August 1993 to July 1995. His research interests include performance evaluation, asynchronous transfer mode (ATM) networks, and personal communication service (PCS) networks.

Dr. Chang is a member of the Chinese Institute of Engineers (CIE).

Chih-Hen Lin received the B.E. and the M.E. degrees in communication engineering from National Chiao Tung University, Hsinchu, Taiwan, R.O.C., in 1992 and 1994, respectively.

Since 1994, he has been an Assistant Design Engineer in the Switching Technology Department, Chunghwa Telecommunication Laboratories, Chungli, Taiwan, R.O.C., where he was involved in constructing and testing the ATM broad-band network.

Da-Sheng Guan received the B.E. and the M.E. degrees in communication engineering from National Chiao Tung University, Hsinchu, Taiwan, R.O.C., in 1992 and 1994, respectively.

Since 1994, he has been an Assistant Design Engineer in the Network Planning Department, Chunghwa Telecommunication Laboratories, Chungli, Taiwan, R.O.C., where he was involved in designing the call control procedure of ISDN PABX. He is currently involved in the software design of the Layer 3 protocol of the wireless subscriber module (WSM) in the personal communications test platform (PCTP) system and the call control procedure of the PCTP system.

Ray-Guang Cheng (S'94–M'97) received the B.E., M.E., and Ph.D. degrees from National Chiao Tung University, Hsinchu, Taiwan, R.O.C., in 1991, 1993, and 1996, respectively, all in communication engineering.

His current research interests include performance analysis, ATM networks, fuzzy systems, and neural networks.

Dr. Cheng is a member of Phi Tau Phi.